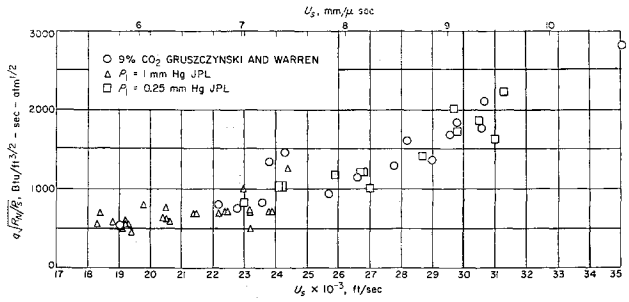

Fig. 2 Stagnation-point heat transfer 9% CO_2, 90% N_2, and 1% A.

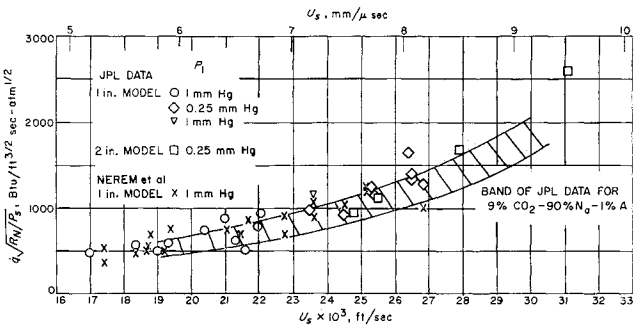

Fig. 3 Convective heat transfer in 100% carbon dioxide.

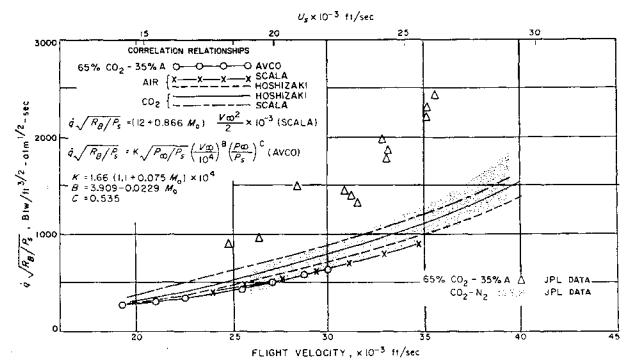

Fig. 4 Convective heat transfer in 65% CO_2 and 35% A.

available on the effect of argon on convective heat transfer in the given velocity range. A large increase in convective heat transfer over that of air-CO_2 mixtures is shown. Thus at 25,000 fps, which is approximately the entry velocity for Mars, there is approximately a twofold increase in the convective heat transfer. Comparison is made also with semi-empirical predictions by Scala[7] and Avco[8] for convection with varying molecular weight. A further comparison is given with the theoretical predictions of Hoshizaki.[9] Good agreement is obtained for air CO_2-N_2 mixtures, but there is a large difference between theory and experiment in the case of argon.

No correction has been made to the data for additional heat transfer due to radiation. This correction is less than 10% for the high velocity data points.

In summary, the carbon dioxide and nitrogen atmospheres have convective heat-transfer rates similar to that of air. The presence of argon in the atmosphere increases the convective heat transfer by about a factor of 2 for the model atmosphere investigated.

References

[1] Kaplan, L. D., Munch, G., and Spinrad, H., "An analysis of the spectrum of Mars," Astrophys. J. **139** (January 1964).

[2] Collins, D. J., Livingston, F., Babineaux, T., and Morgan, N., "Hypervelocity shock tube," Jet Propulsion Lab. TR 32-620 (June 1964).

[3] Rose, P. H., "Development of the calorimeter heat transfer gauge for use in shock tubes," Rev. Sci. Instr. **29**, 557–564 (1958).

[4] Rose, P. H. and Stankevics, J. O., "Stagnation-point heat transfer measurements in partially ionized air," AIAA J. **1**, 2752–2763 (1963).

[5] Gruszczynski, J. S. and Warren, W. R., "Experimental heat transfer studies of hypervelocity flight in planetary atmospheres," AIAA Preprint 63-450 (August 1963).

[6] Nerem, R. M., Morgan, J. C., and Graber, B. C., "Hypervelocity stagnation point heat transfer in a carbon dioxide atmosphere," AIAA J. **1**, 2173–2175 (1963).

[7] Scala, S. M., "The hypersonic environment heat transfer in multicomponent gases," Aerospace Eng. **22**, 10–22 (January 1963).

[8] "Mars-Venus capsule parameter study," Research and Advanced Development Div., Avco Corp., RAD-TR-61-1, Vol. 1, pp. 78–81 (March 1964).

[9] Hoshizaki, H., "Heat transfer in planetary atmospheres at super-satellite speeds," ARS J. **32**, 1544–1552 (1962).

Some Dimensional Considerations of Studies in Space-Flight Simulation

KULDIP P. CHOPRA*
Melpar, Inc., Falls Church, Va.

IT is the attainment of the low-density, high-Mach-number and high-temperature flow conditions, and not merely the attainment of very low density, that poses the real problem in the simulation studies of the flight of objects in the earth's upper atmosphere and outer space. This may be regarded as some advantage in the sense that, under certain conditions as those discussed in this note, it is not necessary to exactly duplicate in the laboratory model studies the low densities encountered in space flight. For example, if the characteristic length of the model l_{mo} bears a ratio α to the corresponding length l of the prototype, the corresponding ratio of the gas densities would be $1/\alpha$ provided that the chemical composition, degree of ionization, and temperature are maintained identically equal in the two situations. In this note, the principle of dimensional similitude is applied to the laboratory model studies of the motion of bodies in an ionized atmosphere pervaded by a magnetic field, and the correspondence relationships for the various characteristic parameters in the actual and model cases are obtained. It is then shown that the scaling relationships satisfy the conditions for aerodynamic, magnetohydrodynamic, and electrodynamic similitude. Such studies are important for the design of instrumentation for diagnostics and the understanding of the dynamics of bodies in space, the interpretation of data on space environment, and the nature of the object-space interactions.

Let us designate the physical parameters in the model experiment by the subscript mo and introduce the scaling factor

$$\alpha = l_{mo}/l \tag{1}$$

and assume that the fractional chemical composition, degree of ionization (n_e/n_0), kinetic temperature T, and flow speed V are identically equal in the two situations. Then,

$$\frac{n_e}{n_0} = \left(\frac{n_e}{n_0}\right)_{mo} \qquad T = T_{mo} \qquad V = V_{mo} \tag{2}$$

where n_e and n_0 are the number densities of charged and

Received July 7, 1964.

* Senior Scientist, Space Science Research Center. Member AIAA.

neutral particles. Since the velocity of sound $c \propto T^{1/2}$, it follows from Eq. (2) that

$$c = c_{mo} \tag{3}$$

Furthermore, the dimensional similarity between the model and prototype situations requires all characteristic lengths, viz., mean free paths and radii of gyration, to be reduced in proportion to the reduction in the linear size of the object. Therefore, Eqs. (1) and (2) yield

$$\frac{n_e}{(n_e)_{mo}} = \frac{n_0}{(n_0)_{mo}} = \frac{\rho}{\rho_{mo}} = \frac{P}{P_{mo}} = \frac{\lambda_{mo}}{\lambda} = \alpha \tag{4}$$

where ρ, P, and λ stand for density, pressure, and mean free path, respectively.

Aerodynamic Similitude

The aerodynamic behavior of the motion of a body is usually described in terms of the characteristic parameters of the flow:

Mach Number

$$M \triangleq V/c \tag{5}$$

Reynolds Number

$$R \triangleq \rho(lV/\eta) \tag{6}$$

Knudsen Number

$$K \triangleq \lambda/l \tag{7}$$

where η is the coefficient of viscosity. The Mach number determines the subsonic, sonic, or supersonic nature of the aerodynamic motion. The Reynolds number determines the relative significance of the intertial and viscous effects. The fluid flow, with predominant viscous effects, is better described by the Knudsen number than by the Reynolds number.

To simulate the true nature of the aerodynamic motion of the body in space, it is necessary to maintain the identity of the characteristic parameters of the fluid flow in the two situations. Equations (2, 3, and 5) yield

$$M/M_{mo} = (V/V_{mo})(c_{mo}/c) = 1 \tag{8}$$

whereas Eqs. (1, 4, and 7) lead to

$$K/K_{mo} = (\lambda/\lambda_{mo})(l_{mo}/l) = 1 \tag{9}$$

Since $\eta \propto \rho\lambda T^{1/2}$, it follows from Eqs. (2) and (4) that

$$\eta = \eta_{mo} \tag{10}$$

Finally, on combining Eqs. (1, 2, 4, 7, and 10), we obtain

$$R/R_{mo} = (\rho/\rho_{mo})(l/l_{mo})(V/V_{mo})(\eta_{mo}/\eta) = 1 \tag{11}$$

Hence,

$$M/M_{mo} = K/K_{mo} = R/R_{mo} = 1 \tag{12}$$

insures the dimensional similitude of the model and the prototype.

Magnetohydrodynamic Similitude

In the presence of a pervading magnetic field H, a charged particle gyrates around a magnetic line of force with a radius $r_c = mv_\perp/eH$, where $v_\perp$ is the component of the particle's velocity in a direction normal to the magnetic field. To reproduce the effects of the pervading magnetic field of the space in the laboratory, the magnitude of r_c must be appropriately reduced such that

$$r_c/(r_c)_{mo} = l/l_{mo} = \lambda/\lambda_{mo} = 1/\alpha \tag{13}$$

This can be achieved by adopting a laboratory magnetic field of strength H_{mo} given by

$$H_{mo}/H = r_c/(r_c)_{mo} = 1/\alpha \tag{14}$$

The last equation combined with Eq. (4) provides

$$H/\rho = (H/\rho)_{mo} \tag{15}$$

which is an important parameter in compressible magnetohydrodynamics[1,2] and is a direct consequence of the well-known frozen-in field concept.

The magnetohydrodynamic coupling is characterized by the Hartmann number

$$\mathcal{H} = Hl(\sigma/\eta)^{1/2} \tag{16}$$

which determines the relative significance of the electromagnetic force σH^2V and the viscous force $\eta V/l^2$, where σ is the electrical conductivity. Since $\sigma \propto T^{3/2}$, it follows from Eq. (2) that

$$\sigma = \sigma_{mo} \tag{17}$$

Substitutions from Eqs. (1, 10, 14, and 17) in (16) yields

$$\mathcal{H} = \mathcal{H}_{mo} \tag{18}$$

When viscous effects are not important, the stringent parameter for the description of magnetohydrodynamic processes is the ratio

$$\mathfrak{N} = \sigma H^2 l/\rho V \tag{19}$$

of the electromagnetic force σH^2V and the inertial force $\rho V^2/l$. Equations (1, 4, 14, and 19) together lead to

$$\mathfrak{N} = \mathfrak{N}_{mo} \tag{20}$$

Hence, the requirements for the dimensional similitude for magnetohydrodynamic phenomena, viz.,

$$\frac{\mathcal{H}_{mo}}{\mathcal{H}} = \frac{\mathfrak{N}_{mo}}{\mathfrak{N}} = \frac{(H/\rho)_{mo}}{(H/\rho)} \tag{21}$$

are satisfied for the adopted scaling relationships. With these parameters, the scaling relationships for the Alfvén speed $V_A = (H^2/4\pi\rho)^{1/2}$ and the cyclotron frequency $w_c = eH/m$, obtained from Eqs. (4) and (14), are the following:

$$V_A/(V_A)_{mo} = \alpha^{1/2} \qquad \omega_c/(\omega_c)_{mo} = \alpha \tag{22}$$

Electrodynamic and Electrohydrodynamic Similitude

The physical parameters in electrodynamics and electrohydrodynamics of an object in an ionized environment are the charged particle mean free path $\lambda_c \propto n_e^{-1}$, Debye shielding distance $\lambda_D \propto (T/e^2n_e)^{1/2}$, plasma frequency $\omega_p \propto (e^2n_e/m)^{1/2}$, the electric potential φ at the object's surface, and the impact parameter $b \propto el\varphi/T$. It follows from Eqs. (2) and (4) that

$$\frac{(\lambda_c)_{mo}}{\lambda_c} = \alpha \qquad \frac{(\lambda_D)_{mo}}{\lambda_D} = \alpha^{1/2} \qquad \frac{(\omega_p)_{mo}}{\omega_p} = \alpha^{-1/2} \tag{23}$$

It is interesting to note that the product of ω_p and λ_D should equal the velocity of sound and obtain identically equal values in the actual and model situations in agreement with Eq. (3).

Again, the surface potential φ depends[3] upon the kinetic temperature of the surrounding plasma and the particle mass, and hence we have

$$\varphi_{mo}/\varphi = 1 \qquad b_{mo}/b = \alpha \tag{24}$$

One test of these scaling relationships would be to check on the stringent ratio

$$\mathfrak{L} = (1/T)(n_e/n_0)(\varphi/V)^2 \tag{25}$$

of the electrodynamic (or electrohydrodynamic) drag force $\propto n_e(l\varphi)^2/T$, and the aerodynamic drag force $\propto n_0l^2V^2$. It readily follows from Eqs. (2, 24, and 25) that

$$\mathfrak{L} = \mathfrak{L}_{mo} \tag{26}$$

and hence these scaling relationships satisfy the conditions for similitude.

Conclusions and Summary

Scaling relationships for the various characteristic parameters of the rapid motion of objects in ionized media pervaded by a magnetic field are obtained. It is seen that, if we relate all characteristic lengths (e.g., size of the object, particle mean free paths, cyclotron radii, etc.) in the laboratory experiment to the corresponding lengths in the actual flight situation by a scaling factor $\alpha = l_{mo}/l \ll 1$, then the pressure, density, magnetic field, and cyclotron frequency must equal $1/\alpha$ times their corresponding values in the actual case, provided that the mean flow speed, chemical composition, kinetic temperature, and degree of ionization are identical in the two situations. With these scaling relationships for the various parameters, the Mach number, the Knudsen number, the Reynolds number, the Hartmann number, and the ratios (H/ρ) and (coulomb drag/aerodynamic drag) are maintained identically equal in the model and the prototype, thereby satisfying the conditions of dimensional similitude. The Alfvén speed and plasma frequency are higher in the laboratory by a factor $\alpha^{-1/2}$ whereas the Debye length is lower by a factor of $\alpha^{1/2}$. These relationships are also in agreement because their product equals the speed of sound, which has identically equal values in the two situations.

References

[1] De Hoffman, F. and Teller, E., "Magnetohydrodynamic shock waves," Phys. Rev. **80**, 692 (1950).

[2] Chopra, K. P., "Some problems in hydromagnetics," Univ. of Southern California Engineering Center TN56-205, Air Force Office of Scientific Research AFOSR-TN-59-265 (1959).

[3] Chopra, K. P., "Interactions of rapidly moving objects in terrestrial atmosphere," Rev. Mod. Phys. **33**, 153 (1961).

Propellant Potential of Vaporized Metals in Temperature-Limited Rocket Systems

I. Glassman,* R. F. Sawyer,† and A. M. Mellor‡
Princeton University, Princeton, N. J.

In temperature-limited rocket propulsion systems such as electrothermal jet engines, solid core nuclear rockets, radioisotope rockets (Poodle), etc., it is accepted fundamentally that hydrogen is the best propellant because of its high enthalpy per unit mass. However, if one considers the latent heat of vaporization (condensation, sublimation) as another thermal degree of freedom, then it can be shown theoretically that the combination§ of the light metallic elements with hydrogen can surpass hydrogen in performance. In particular, it can be established that under space conditions the storable compound pentaborane is superior to cryogenic hydrogen. The result is possible because of the high heat of vaporization of boron, 11.2 kcal/g.

Received August 13, 1964. The concept reported here was developed while work was being performed under metal combustion studies supported by NASA Grant NsG641 and chemical kinetic studies supported by Air Force Office of Scientific Research Contract AF49(638)-1268.

* Professor, Department of Aerospace and Mechanical Sciences, Guggenheim Laboratories for the Aerospace Propulsion Sciences. Associate Fellow Member AIAA.

† Assistant-in-Research, Department of Aerospace and Mechanical Sciences, Guggenheim Laboratories for the Aerospace Propulsion Sciences. Member AIAA.

‡ Assistant-in-Research, Department of Aerospace and Mechanical Sciences, Guggenheim Laboratories for the Aerospace Propulsion Sciences. Student Member AIAA.

§ The word combination is used here to mean a liquid hydride, any dispersion of metal particles in liquid hydrogen, liquid hydrogen and a gel containing metal particles, etc.

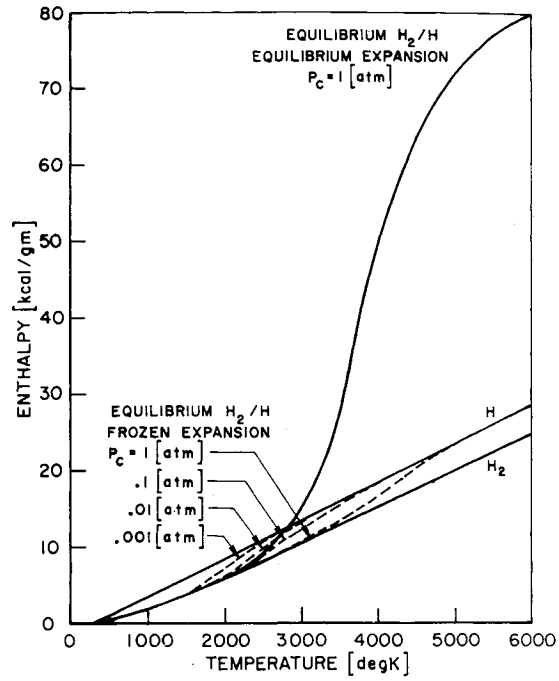

Fig. 1 Hydrogen enthalpies. Equilibrium[2] and frozen[3] expansion to 298°K.

Jack[1] was the first to consider the possible use of the light metallic elements as propellants in electrothermal jet engines. However, he restricted himself to a single metallic element as a working fluid. Dealing mainly with lithium because of its low atomic weight, he expressed concern whether condensation was desirable because of the formation of condensation shocks and the lack of a working fluid. The approach offered here differs from that of Jack in that the light metallic elements always are used in association with hydrogen as a carrier fluid. More important, though, it is argued that condensation is desirable and will take place some time during the nozzle expansion process. This assumption seems valid when one realizes that a complex condensed oxide like Al_2O_3 can be formed from suboxides and oxygen in rocket motors whose chamber temperatures are substantially higher than those found in temperature-limited systems.

The major assumptions and points are developed by describing the two figures. In Fig. 1 the available enthalpy per gram of various possible hydrogen systems is plotted. The square root of this enthalpy is, of course, directly proportional to the specific impulse. The S-shaped curve describes the available enthalpy for a hydrogen system heated to the temperature designated on the ordinate. The equilibrium dissociation of hydrogen is calculated at 1-atm total pressure. The H_2/H mixture obtained is expanded to the thermodynamic base temperature 298°K, and equilibrium is considered to be held throughout the expansion. Since the enthalpy at 298°K is the exhaust enthalpy, the curves represent the enthalpy available for propulsive work. The curves labeled H and H_2 are the sensible enthalpy of hydrogen atoms and molecules, respectively. The dotted lines represent the available enthalpy for equilibrium dissociation of H_2 and frozen expansion flows. From the kinetic recombination rates of H atoms, it appears that high-temperature H atom nozzle flows are essentially frozen. Consequently, comparisons here will be made with the lower set of curves in Fig. 1, and the dashed ones in particular.